# Toxicity and developmental effects of Arctic fuel oil types on early life stages of Atlantic cod (*Gadus morhua*)

Bjørn Henrik Hansen [a,*], Trond Nordtug [a], Julia Farkas [a], Essa A. Khan [b], Erika Oteri [b], Bjarne Kvæstad [a], Liv-Guri Faksness [a], Per S. Daling [a], Augustine Arukwe [b]

[a] *SINTEF Ocean, Climate and Environment, Trondheim, Norway*
[b] *Norwegian University of Science and Technology, Department of Biology, Trondheim, Norway*

ABSTRACT

Due to the heavy fuel oil (HFO) ban in Arctic maritime transport and new legislations restricting the sulphur content of fuel oils, new fuel oil types are continuously developed. However, the potential impacts of these new fuel oil types on marine ecosystems during accidental spills are largely unknown. In this study, we studied the toxicity of three marine fuel oils (two marine gas oils with low sulphur contents and a heavy fuel oil) in early life stages of cod (*Gadus morhua*). Embryos were exposed for 4 days to water-soluble fractions of fuel oils at concentrations ranging from 4.1 - 128.3 μg TPAH/L, followed by recovery in clean seawater until 17 days post fertilization. Exposure to all three fuel oils resulted in developmental toxicity, including severe morphological changes, deformations and cardiotoxicity. To assess underlying molecular mechanisms, we studied fuel oil-mediated activation of aryl hydrocarbon receptor (Ahr) gene battery and genes related to cardiovascular, angiogenesis and osteogenesis pathways. Overall, our results suggest comparable mechanisms of toxicity for the three fuel oils. All fuel oils caused concentration-dependant increases of *cyp1a* mRNA which paralleled *ahrr*, but not *ahr1b* transcript expression. On the angiogenesis and osteogenesis pathways, fuel oils produced concentration-specific transcriptional effects that were either increasing or decreasing, compared to control embryos. Based on the observed toxic responses, toxicity threshold values were estimated for individual endpoints to assess the most sensitive molecular and physiological effects, suggesting that unresolved petrogenic components may be significant contributors to the observed toxicity.

## 1. Introduction

Due to continuous withdrawal of the Arctic sea ice, there has been and will continue to be increased maritime activity and transportation in the Arctic region. New international regulations restricting the sulphur content of fuel oils onboard vessels have driven the refinery industry to manufacture new fuel products that comply with international, as well as local, policies. As these different products have varying chemical, physical and toxicological properties, their fate and potential effects in the environment in the event of accidental spills will inevitably vary. In the unfortunate event of an accidental spill, it is important to have in-depth knowledge about how the specific spilled oil will behave and affect local populations and ecosystems, and how to reduce these impacts through oil spill response contingency and planning.

Heavy fuel oils (HFO), which is a residue from crude oil distillation and cracking, is the main type of bunker oil used by large vessels in maritime transportation. HFO is highly viscous, contains high levels of paraffins, cycloparaffins, aromatics, olefins, and asphaltenes as well as heterocyclic compounds containing sulfur, oxygen, nitrogen and/or organometals. When accidentally released into the marine environment, HFO will form highly viscous and stable emulsions which will cause environmental damage especially if reaching shoreline habitats. A HFO ban in Arctic areas have been debated for years (DeCola et al., 2018; Prior and Walsh, 2018), but currently only very few areas have implemented an HFO-ban, e.g. in specific nature reserves and national parks around Svalbard, Norway, only light distillate DMA quality fuel oils (ISO 8217: 2017 standard) are allowed onboard boats (Lovdata, 2014). In the event of accidental spills to the marine environment, such low viscous, light distillates will, compared to HFO, have a reduced "lifetime" (persistence) on the sea surface due to higher degree of natural dispersion into the water column leading to increased microbial biodegradation. The global requirements for marine fuel oils are governed by

---

* Corresponding author.
*E-mail address:* bjorn.h.hansen@sintef.no (B.H. Hansen).

International Convention for the Prevention of Pollution from Ships (MARPOL), and focusses primarily on reducing the global emissions of sulphur oxide (SOx) and nitrogen oxide (NOx) from vessels. Global requirements have reduced from 4.5 to 3.5% sulphur in 2012 and down to 0.5% sulphur (very low sulphur fuel oil, VLSFO) in 2020. For Sulphur Emission Control Areas (SECA), like the North Sea, the Baltic Sea and the east and west coast of USA and Canada, the limits set out in Annex VI of the MARPOL Convention was reduced from 1% to 0.10% sulphur (ultralow sulphur fuel oil, ULSFO) in 2015. Importantly, the MARPOL Convention currently only restricts the sulphur content of oil, not the other properties affecting their fate and effects during accidental spills to the marine environment. The low sulphur-requirements from the MARPOL Convention have led to new fuel products entering to the market, and these refined products can be light distillates, heavy distillates or residual fuel oils, thus varying tremendously in terms of physical, chemical and toxicological properties. However, they need to be compliant with regulations for the area they are being transported, so for the Svalbard area only light distillates (DMA) with <0.5% sulphur content can be used.

In the event of acute oil spills from maritime transport, it is important to know how the properties of the spilled fuel oils affect their fate in the sea and their potential impact on local biota. The expected environmental benefit from using light distillates, like DMA, compared to HFO is primarily based on their shorter 'life-time' on the sea surface. For pelagic marine organisms, however, the lighter properties of DMA may not be favourable as these fuel oils will be more dispersible and contain higher levels of water-soluble and potentially toxic components. In a toxicity study of water accommodated fractions (WAFs) of six different marine fuel oils, including light distillates, heavy distillates, and different residual fuel oils, on marine algae (*Skeletonema costatum*) and copepods (*Calanus finmarchicus*), a DMA-quality marine diesel was the most acutely toxic (Hellstrøm, 2017). In addition to these acute effects, water-soluble components of petrogenic oil have been shown to produce sub-lethal toxicological responses, such as aryl hydrocarbon receptor (Ahr) activation and other adverse effects related to bone quality and cardiovascular dysfunction in fish species (Arukwe et al., 2008; Esbaugh et al., 2016; Hansen et al., 2018a, 2019a, 2019b; Incardona et al., 2014; Incardona and Scholz, 2016; Olufsen and Arukwe, 2011; Scott et al., 2011). The Ahr is a member of the basic helix-loop-helix-PAS (bHLH-PER-ARNT-SIM) family of gene regulatory proteins (Josyula et al., 2020) that play important roles in xenobiotic toxicity and developmental processes (Watson et al., 2019). Some components of crude oils, particularly 4 - 5 ringed PAHs, such as benzo(k)fluoranthene and indeno[1,2,3-*cd*]pyrene (Barron et al., 2004; Billiard et al., 2002), act as ligands for the Ahr, which subsequently dimerizes with Ahr nuclear translocator (Arnt) to form a complex that translocate to the nucleus where it transactivates mRNA transcription of genes containing xenobiotic or dioxin response elements (XREs or DREs) in their upstream regions (Gu et al., 2000). The molecular action of the Ahr is regulated by the Ahr repressor (Ahrr) through a negative feedback mechanism (Gu et al., 2000; Josyula et al., 2020). Despite the classical roles of Ahr in xenobiotic metabolism, it also plays significant roles in several developmental processes, cardiovascular function and interactions (or crosstalk) with hormonal systems and transforming growth factor b (Tgf-b) has been reported (Gomez-Duran et al., 2009; Watson et al., 2019). There is a need to supplement these studies with toxicity tests at higher trophic levels. Early life stages of fish have been shown to be particularly sensitive to oil exposure (Hansen et al., 2018a; Sørhus et al., 2015) and it is necessary to establish toxicity threshold values for such organisms. Threshold toxicity values for different organisms are essential inputs for predicting potential adverse effects associated with accidental releases, as well as evaluating response actions that must be initiated after accidental spills.

Therefore, the aim of the current study was to evaluate the harmful effects of different marine fuels on sensitive life stages of fish in marine Arctic waters. We have used two DMA quality marine gas oils (MGO500

and MGO1000) with different sulphur content (SI1, Table S1.1) and a heavy fuel oil (IFO-LS) as a reference. Standard low-energy WAFs (LE-WAFs) were prepared, diluted and utilized for exposing cod embryos for four days, followed by a recovery period in clean seawater until day 17 dpf. Our hypothesis are - (a) that embryonic exposure to fuel oils will activate Ahr gene battery in the biotransformation and developmental pathways, and (b) fuel oil mediated activation of Ahr gene battery will produce downstream consequences related to developmental toxicity, cardiovascular, angiogenesis and osteogenic differentiation that alter the morphology and general health of cod larvae. Based on the toxicological responses observed after exposure, toxicity threshold values will be estimated for individual endpoints to assess the most sensitive molecular and physiological effects.

## 2. Materials and methods

### 2.1. Choice of marine fuels

Three marine fuel oils were chosen for the present study, namely marine diesel from the Rotterdam refinery, marine gas oil from Esso Slagen and heavy fuel oil (IFO 180) supplied by the Coastal Authorities of Norway. The marine diesel and gas oils were both DMA quality, and identified here as MGO1000 and MGO500, respectively. The heavy fuel oil is referred to as IFO-LS. The fuel oils were used as fresh products. Different properties of the marine fuel oils used in this study are presented in Table S1.1 of the supplementary information (SI 1) file.

### 2.2. Preparation of exposure solutions

Low energy WAF (LE-WAF) was prepared according to established guidelines by the Chemical Response to Oil Spills: Ecological Research Forum (CROSERF), with essential details as previously described (Faksness and Altin, 2017) using oil-to water ratio of 1:10 000. LE-WAFs was preferred for this study to avoid the generation of oil droplets, since these may adhere to eggs and subsequently contribute to additional exposure through passive diffusion (Hansen et al., 2018b).

The exposure design was a 96 - h static renewal procedure with supplement of fresh solution after 48 h. To quantify the rate loss of components with time, the highest exposure concentrations were analysed at the start and after 48 h. Median exposure concentrations were then estimated assuming a logarithmic decline in concentration and applying the measured rate to the two 48 h periods before and after supplement with fresh exposure solution (SI 6: Fig. 6.1). See also Table S5.1 (SI 5) for the characterization of initial chemical composition. All data on biological effects are related to estimated median concentration.

### 2.3. Water sampling and chemical analyses

Water samples were taken after WAF generation and after 48 h of exposure. A detailed protocol for chemical analysis is presented in the supplementary information (SI11) file and as previously described (Faksness and Altin, 2017).

### 2.4. Exposure of fish eggs

Eggs and milt from adult Atlantic cod (*Gadus morhua*) were collected through strip-spawning from broodstock fish kept at 9 °C in 7000 L tanks at Austevoll Research Station at the Institute of Marine Research (IMR). Eggs were fertilized in the evening and kept overnight to verify good fertilization (>80%). Fertilized eggs (300 mL, 1 dpf) were then sent to SINTEF Sealab (Trondheim) by airfreight. On arrival, eggs were placed in 50 L tanks with filtered (1 μm) seawater (8 ± 1 °C) in a flow-through system that delivered five volume water exchanges/day. Natural seawater, collected from 80 m depth (below thermocline) at a putatively non-polluted Norwegian fjord (Trondheimsfjord; 63 °26′ N, 10 °23′ E),

was supplied by a pipeline system to our laboratories (salinity of 34‰, pH 7.6). Gentle air bubbling was used to generate continuous embryo movement within the tanks. The embryos were acclimated until 4 dpf when they were transferred to glass beakers for exposure, and at the onset of exposure, the embryos were in gastrulation (reached 100% epiboly). Exposure to crude oil during this developmental period has previously been shown to cause developmental effects on larvae (Hansen et al., 2019a).

The LE-WAFs generated from the three oils were diluted with filtered seawater at nominal concentrations of 6, 12, 25, 50 and 100% solutions. These solutions were transferred to glass jars (100 mL) and used to expose fish eggs (approx. 100 eggs in each jar) for 4 days (4 - 8 dpf). After 2 days of exposure, an additional 100 mL of fresh exposure solution was added to each jar to compensate for the initial loss of oil components. The exposures were performed in four replicates ($n = 4$). At 8 dpf, dead eggs were removed and counted, while the remaining live eggs were moved to clean glass beakers containing clean seawater (100 mL) and maintained at $8 \pm 1$ °C until 16 dpf (recovery period). Survival and hatching were monitored daily during the recovery period.

### 2.5. Estimation of exposure concentration in semi-static system

Using static exposure conditions in open containers is not optimal for generating adequate effect levels. These experiments should preferably be performed in flow-through system. However, due to technical limitations, this was not possible in the current experiments. The chemical analysis of the exposure solutions after 48 h showed a decline in concentration with 76 - 80% compared to the initial concentration for TPAH. Concentration decline in static exposure systems may be due to evaporation, adhesion to glass walls and bioaccumulation in exposed eggs. To reduce this effect, we added fresh exposure solutions after 48 h exposure. However, the initial concentration is not an adequate representation of the exposure situation. To better describe the exposure, we used the measured decline in concentration during the first 48 h and applied that to all exposure solutions, both before and after the addition of fresh solutions. The median concentration was then calculated assuming a logarithmic decline and calculating below the reconstructed exposure curve (SI6: Fig. S6.1).

### 2.6. Gene expression analyses

Total RNA was extracted from 10 embryos sampled from each replicate and treatment at the end of exposure using the Direct-zol™ RNA kit, according to the protocol provided by the manufacturer. RNA quality was confirmed by combined agarose gel electrophoresis and spectrophotometric analysis. Complementary DNA (cDNA) was generated using iScript cDNA synthesis kit (Bio-Rad) and mRNA levels were measured with an Mx3000P quantitative PCR machine (Stratagene, La Jolla, CA). Specific primer pair sequences (SI3: Table S3.1) were used for transcript amplification according to standard protocol (Arukwe 2006). The primer pairs were tested prior to use, showing single amplified product of expected size for individual transcripts. Expression of each mRNA was quantified using a well-validated approach of absolute quantification as previously described (Arukwe 2006) and as presented in SI (SI 12).

### 2.7. Larvae morphology

At 17 dpf, 6 −12 larvae from each replicate were collected and individually immobilized in a glass petri dish filled with 3% methyl-cellulose kept at 8 °C. Images were collected through a microscope (Eclipse 80i, Nikon Inc., Japan) quipped with Nikon PlanApo objectives (2x for whole larvae images and 10x for close-up larvae images and videos), a 0.5x video adaptor and CMOS camera (MC170HD, Leica Microsystems, Germany). Standardised images of larvae were used for analyses of standard length, body area, yolk-sac area, myotome height,

eye area and eye-to-forehead distance. This analysis, as descibed in detail in Kvæstad et al. (submitted), was automated using deep learning with mask R-CNN neural net architecture (He et al., 2017) trained on 183 manually annotated images of cod larvae at different dph. The neural net architecture outputs outline of the body, eye and yolk, where measurements such as area and length were calculated using automated image processing techniques such as Topological Structural Analysis (TSA) (Suzuki, 1985), ellipse fitting (Fitzgibbon and Fisher, 1996) and skeletonize (Zhang and Suen, 1984). Representative images of larvae with highlighted traces of distance/area are given in Fig. 1A.

Blinded deformation ranking analysis of imaged larvae was performed by methods adopted from Sørhus et al. (2015) and Hansen et al. (2018a). The degree of selected morphological abnormalities (jaw deformations, craniofacial deformations, pericardial oedema and spine deformations) were determined for larvae (17 dpf) according to a scale of 1 - 3 (where 1 is normal, 2 is moderate, and 3 is severe deformation) (Hansen et al., 2018a, 2019b; Sørensen et al., 2019; Sørhus et al., 2015). Example of control and deformed larvae are given in Fig. 1B-G.

### 2.8. Cardiac activity

Videos taken through the microscope were used as a basis for monitoring heart rate (HR) in individual larvae using automated video analyses (Nepstad et al., 2017). Briefly, this method uses image processing and statistical techniques to extract HR information from microscopy videos at the larval stages. The method enables automatic processing for many individuals, while simultaneously eliminating common errors that might occur during manual processing. Lack of ventricle constriction (silent ventricle) was also assessed for all larvae, and severity degrees were assigned where 0 was normal ventricle constriction and 3 was assigned when there was no constriction of the ventricle.

### 2.9. Data analysis

Statistical analyses were conducted using GraphPad Prism statistic software, V6.00 (GraphPad Software, Inc., CA, USA). Depending on the data sets, statistical analyses were performed by comparing exposed groups to control groups using (data normally distributed) ANOVA followed by Dunnett's post hoc test, ANOVA followed by Kruskal-Wallis non-parametric test (data not normally distributed), or Brown-Forsythe and Welch ANOVA tests. The latter was used for hatching time (T50) only, where mean hatching time (and associated SD) was
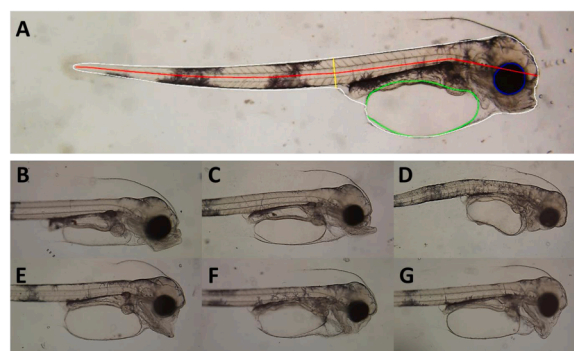


**Fig. 1.** A: Example of a cod larvae with highlighted automated measurements. White, green and blue lines display the area surrounding the body, yolk sac and eye, respectively. The red line displays the standard length and yellow line represents the myotome height. B-G: Examples of a cod larvae with deformations. B: Normal cod larvae. C: Jaw deformation severity degree (JDSD) 2, craniofacial deformation severity degree (CD) 3, pericardial oedema (PE) severity degree 2 and spine deformation (SD) severity degree 0. D: JD 3, CD 3, PE 0, SD 1. E: JD 3, CD 2, PE 0, SD 0. F: JD 3, CD 3, PE 3, SD 0. G: JD 3, CD 3, PE 3, SD 0.

provided by non-linear curve fit of accumulated hatched larvae as a function of time (days after fertilization). The significance level was set at $p < 0.05$ unless otherwise stated. Nonlinear curve fit (third-order polynomial) was used in figures displaying effects as a function of exposure.

## 3. Results

### 3.1. Chemical characterization of fuel oil LE-WAFs

The LE-WAFs of the three fuel oils differ in their chemical composition (Fig. 2). The total WAF concentrations measured as the sum of volatile organic components (VOC, C5 - C9) and total extractable material (TEM) differed significantly. MGO1000 was the highest and represents double the concentrations in the MGO500 and IFO-LS oils (Fig. 2A). IFO-LS had only miscible levels of VOC, which was dominated by BTEX, C3- and C4-benzenes in the two diesels (Fig. 2B). In general, all the oil types had considerable concentrations of semi-volatile organic components (SVOC, Fig. 2C), dominated by naphthalenes, but also with high concentrations of dibenzofuran, acenaphthene, C0 - C1-phenanthrenes and fluorenes (Fig. 2C). Low concentrations of heavier PAHs (4 - 6 ring) were observed, reflecting their low water solubility. Overall, the MGO1000 fuel oil displayed the highest concentrations of most identified/resolved and unresolved (UCM) components.

All exposure solutions were analysed for total extractable material (TEM) and SVOC using GC-FID and GC–MS, respectively, at the onset of exposure (SI 4: Table S4.1) and after 48 h, when exposure solutions were renewed. As expected, the concentration series for MGO1000 was at a higher level compared to the other two fuel oils. There was a decline in exposure concentrations over time and the average loss for total PAHs in the highest concentrations after 48 h was 76 – 80% for all fuel oils. This was partly compensated by adding fresh exposure solution after 48 h, so that the estimated median exposure concentrations of TPAH was about 50% of the initial exposure concentrations (SI 5: Table S5.1). Estimated median concentrations (SI 6: Fig. S6.1) were therefore used for establishing effect limits.

### 3.2. Transcript changes of ahr gene battery

Transcript expression for *cyp1a* and *ahrr* expressions showed significant concentration-dependant induction pattern, for all oil types, compared to controls (Fig. 3A and B, respectively). On the other hand, *ahr1b* mRNA did not show any significant exposure related changes in expression patterns. In general, a trend toward decreases in expression levels below control, was observed by the different exposures (Fig. 3C, except IFO-LS at 25%).

### 3.3. Transcript changes for angiogenesis and osteogenic differentiation

Transcripts related to angiogenesis and osteogenic differentiation (*vegfaa, runx2b, osteocalcin, col1a1a, col1a1b, ctsk, bmp4, bmp9* and *osterix*) were analysed. For *vegfaa*, 6% MGO500, MGO1000 and IFO-LS decreased mRNA expression below control levels, and thereafter, the different oil types produced concentration and oil type specific increases of *vegfaa* mRNA, albeit not significant (Fig. 4A).

The *col1a1a* gene was generally decreased by exposure to the different oil types, in a concentration specific manner, except for 12% MGO-500 that increased *col1a1a* mRNA expression (Fig. 4A). On the contrary, *col1a1b* showed concentration-specific decreases after exposure to MGO500 and MGO1000, while IFO-LS produced an apparent concentration-dependant increase of *col1a1b* mRNA, compared to control (Fig. 4C). For *runx2b*, MGO1000 produced a concentration-specific increase of mRNA expression, while MGO500 and IFO-LS produced concentration-specific increase or decrease of mRNA expression, compared to control (Fig. 4D). However, the *runx2b* expression patterns were not significantly different from control.

A unique pattern of effects was observed for *bmp4* and *bmp9* after exposure to the different oil types, by either increasing or decreasing, depending on concentration and oil type (SI 7: Fig. S7.1A and B). Similarly, *osteocalcin* and *osterix* mRNA showed variable expression patterns by either increase or decrease, that was dependant on Arctic oil type or exposure concentration (SI 7: Fig. S7.1C and D).
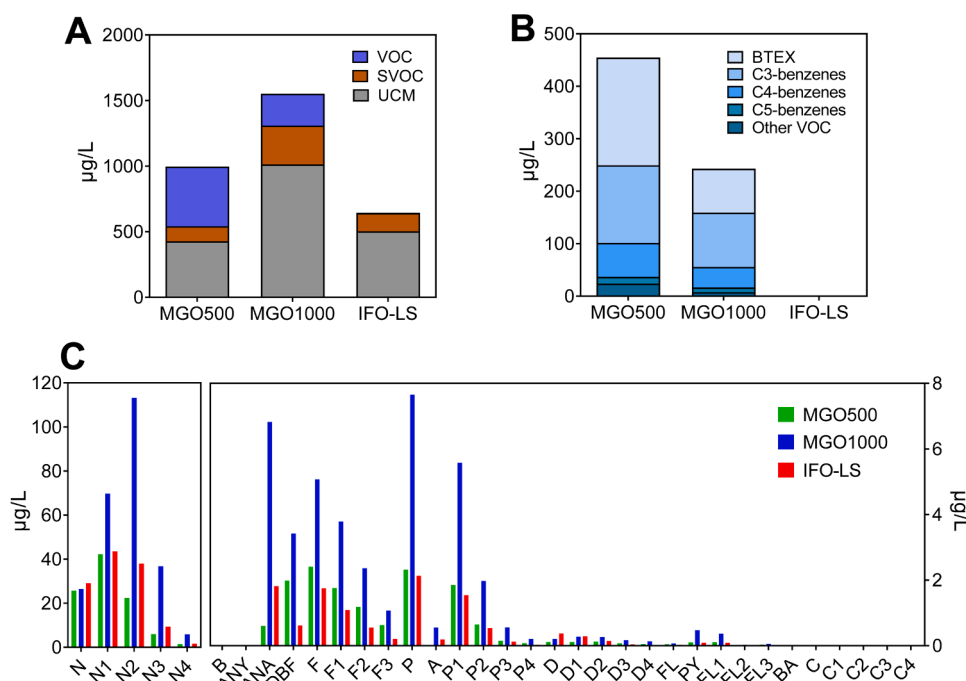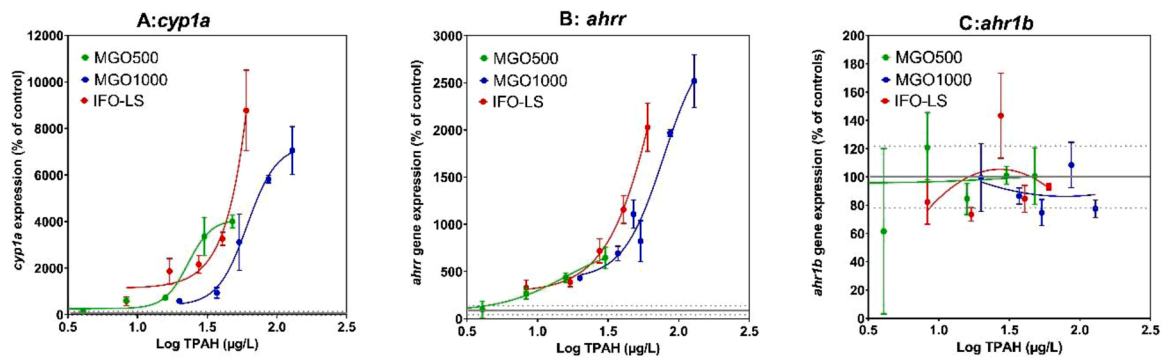


**Fig. 2.** Chemical composition of initial WAFs (100%). A: Separated into VOC, SVOC and unresolved complex material (UCM). B: VOC composition only. C: Speciated composition of individual PAHs. Note different scaling on the axes. All concentrations are given in μg/L.

**Fig. 3.** Expression of genes related to the Ahr pathway in cod embryos exposed to WAFs of MGO500 (green), MGO1000 (blue) and IFO-LS (red). Expression levels (% of controls) are given as mean ± SEM, ($N = 4$ throughout). Control values are given as grey line (broken line: SEM, $N = 4$). A: *cyp1a*. B: *ahrr*. C: *ahr1b*. Note different scaling on the axes.
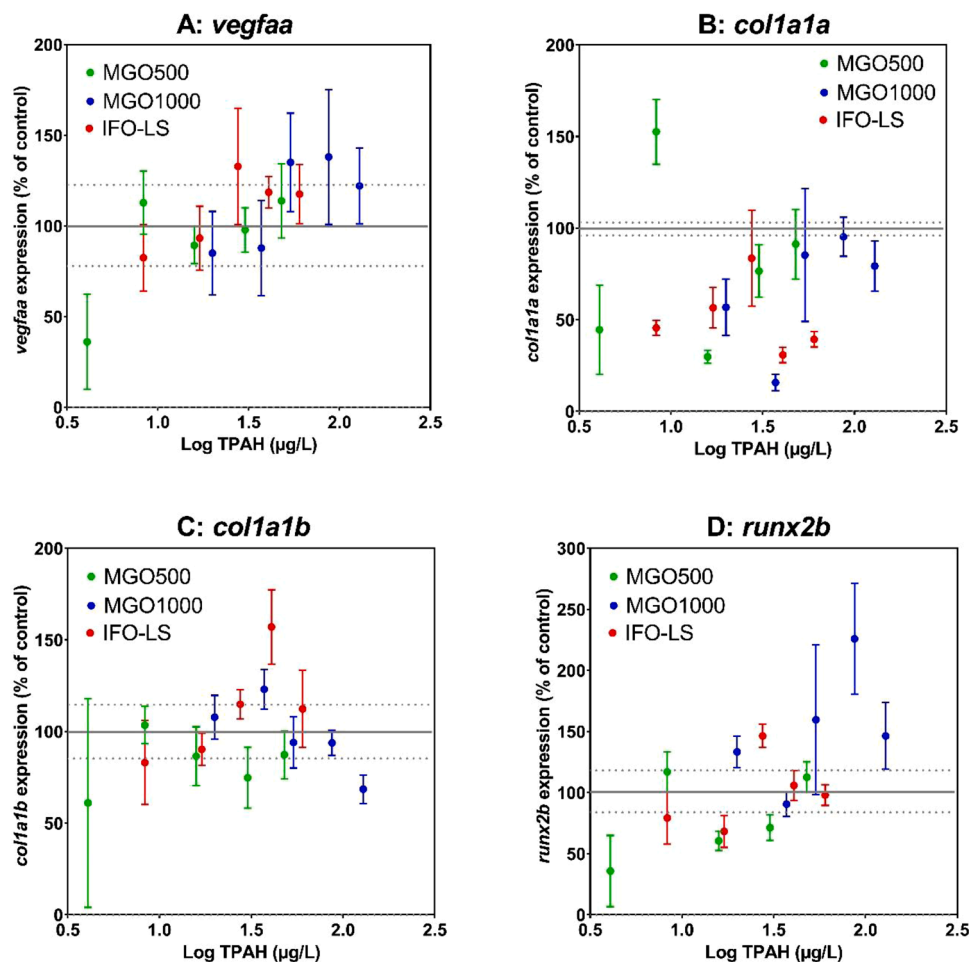


**Fig. 4.** Expression of genes related to the angiogenesis and osteogenic differentiation in cod embryos exposed to WAFs of MGO500 (green), MGO1000 (blue) and IFO-LS (red). Expression levels (% of controls) are given as mean ± SEM, ($N = 4$ throughout). Control values are given as grey line (broken line: SEM, $N = 4$). A: *vegfaa*. B: *col1a1a*. C: *col1a1b*. D: *runx2b*. Note different scaling on the axes.

### 3.4. Hatching and survival

Hatching success was relatively high for all treatments (>80%), and there was no clear relationship with either concentration or oil type (SI 8: Table S8.1). Significant reduction in hatching success was only observed in few exposure groups (MGO500: 12% ($p < 0.01$), 100% ($p < 0.05$), IFO-LS: 100% ($p < 0.001$)). Hatching was significantly ($p < 0.0001$) initiated earlier (premature hatching) in embryos exposed to

fuel oil types, compared to control, but no clear concentration-dependant pattern was observed (SI 8: Table S8.1). For the lowest exposure concentrations, larvae hatched almost 4 days earlier than in controls. Reduced larvae survival was observed for all fuel oil exposures, showing significantly ($p < 0.05$, see SI 8: Table S8.1 and SI 9: Table S9.1 for specific significance levels) lower for MGO500 (6%, 25%, 50%), MGO1000 (6%, 25% and 50%) and IFO-LS (6% and 50%). The relationship between larvae survival and exposure concentrations were

∩-shaped. The monitoring timeframe for larvae were different between exposure groups, due to differences in hatching time. For example, at the lowest exposure concentrations, where larvae hatched 4 days earlier than controls, the cumulative larvae mortality was higher than controls, but they were also monitored as larvae for 4 additional days. Premature hatching may also cause altered growth, yolk utilization (Politis et al., 2014) or reduced survival (Farkas et al., 2021) contributing to the lack of dose-response for survival after exposure to fuel oils. The measurements of survival may also be affected by the larvae behaviour. Particularly, for the high concentrations, larvae were not moving very much, and we had to test for survival using the microscope to observe heart beats. This was, however, done consistently for the highest exposure concentrations only.

### 3.5. Larvae condition

At 17 dpf, larvae for every treatment were imaged, and images were used to assess morphometry, development and deformations. Three standard measures of development; body area, standard length and myotome height, all displayed clear concentration-dependant reductions (Fig. 5A-C). Compared to control performance, body area and myotome height were smaller, but significantly smaller only for larvae exposed to 100% MGO1000 ($p < 0.05$). For larvae standard length, oil types exposed larvae were significantly shorter, compared to control for all exposure concentrations of MGO500, MGO1000 (except 12%) and IFO-LS. The yolk fraction (body area containing the yolk sac) was significantly higher, compared to controls for all treatments (except 6% MGO500 group). This effect was also observed in a concentration-dependant manner for all fuel oils (Fig. 5D). See Table S9.1 (SI 9) for additional statistical information. As larvae were imaged on the same day of post fertilization (17 dpf), we expected that exposure groups that hatched prematurely would display larvae with longer and larger body

size and smaller yolk sacs, compared to controls and those that hatched up to 4 days later. However, this was not the case.

### 3.6. Larvae deformations

Measurements of cranium and jaw region deformations showed that larval eye diameter and deformation severities were affected in an apparent concentration-dependant manner. Smaller eyes and shorter distances between eyes and forehead were observed in larvae after exposure to 100% WAFs of MGO500, MGO1000 and IFO-LS ($p < 0.01$) (Fig. 6A and B). Ranking of craniofacial and jaw deformations based on a system adopted from Sørhus et al. (2015), produced clear concentration-dependent effects (Fig. 6C and D). Statistical analyses showed that, significantly higher ($p < 0.05$) deformation severities were observed for MGO500 (50% and 100%), MGO1000 (50% and 100%) and IFO-LS (100%). See SI 9 (Table S9.1) for additional information regarding statistical significance levels.

### 3.7. Cardiac toxicity

A concentration-dependant reduction (Fig. 7) in larvae heart rate for MGO1000 and IFO-LS was observed, showing significantly lower HR for 50% and 100% MGO1000. A typical cardiotoxic appearance of a non-functional ventricle, so-called 'silent ventricle', was evident (Fig. 7B) and significantly so, in hatched larvae from the MGO500 100%, MGO1000 50% and 100%, and IFO-LS 100% ($p < 0.0001$) exposure groups. The occurrence and severity of pericardial oedema were also assessed in all sampled larvae (Fig. 7C), showing significantly higher ($p < 0.0001$) severities in 100% MGO500, 50% and 100% MGO1000 and 100% IFO exposure groups.
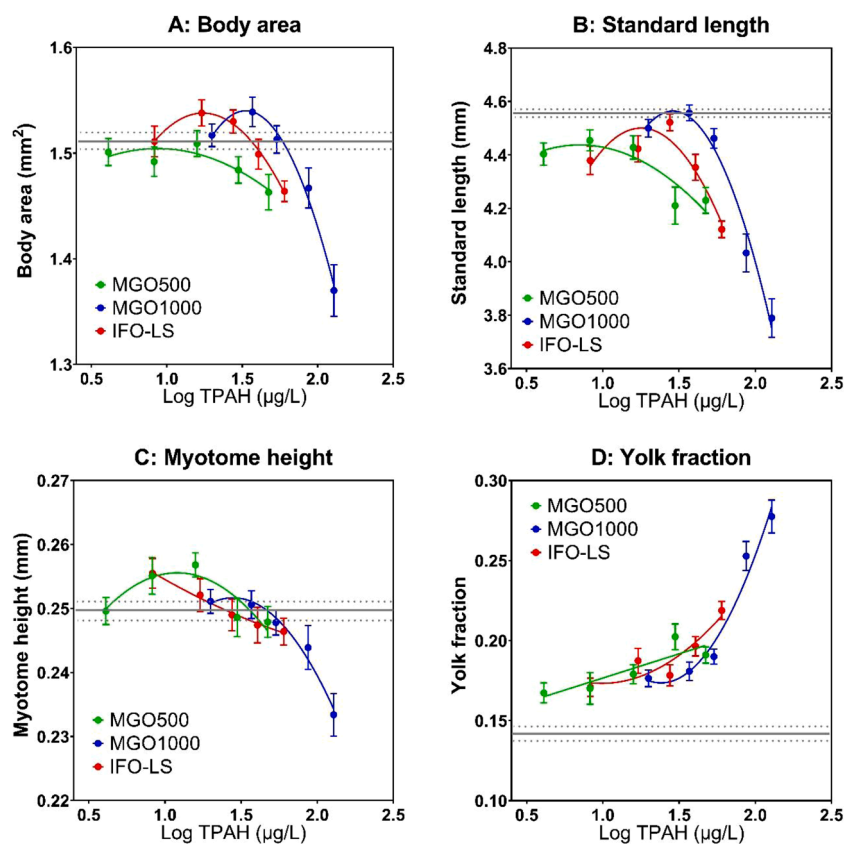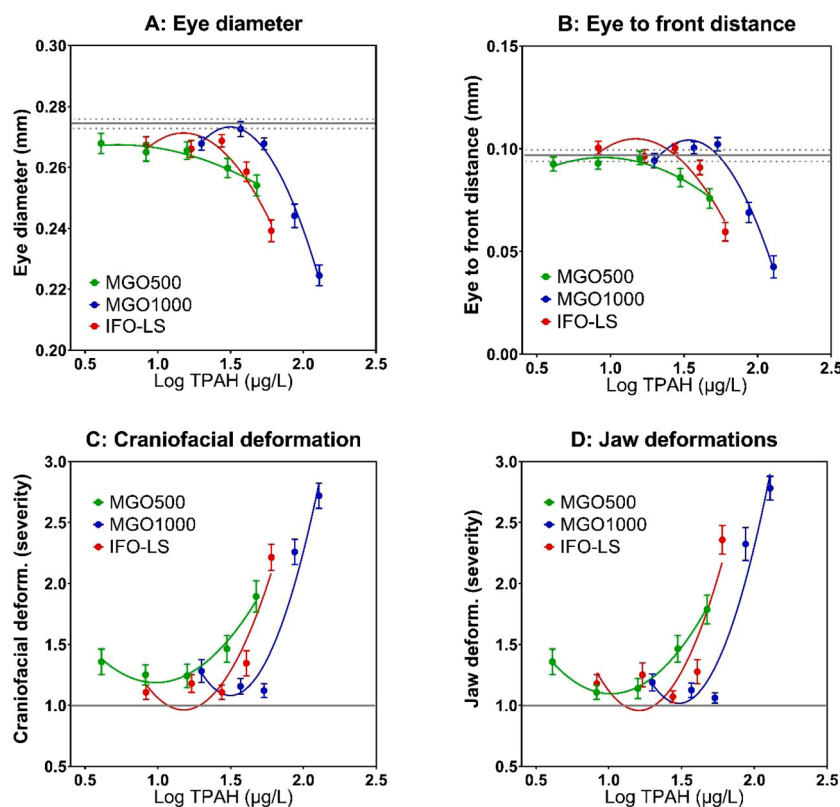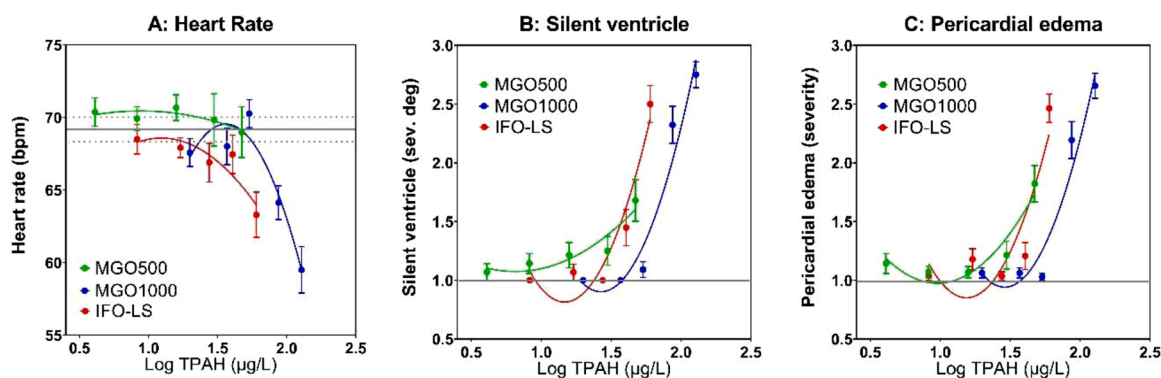


**Fig. 5.** Developmental data on cod larvae exposed MGO500 (green), MGO1000 (blue) and IFO (red) as a function of exposure concentration (μg/L TPAH). Data given as average ± SEM ($N = 28 - 32$). Control values are given as grey line (broken line: SEM, $N = 45$).

**Fig. 6.** Deformation data of cod larvae exposed to MGO500 (green), MGO1000 (blue) and IFO (red) as a function of exposure concentration (µg/L TPAH). A: Eye diameter. B: Distance between eye and forehead. C: Craniofacial deformation severity. D: Jaw deformation severity. Data given as average ± SEM ($N = 28 - 32$). Control values are given as grey line (broken line: SEM, $N = 45$).



**Fig. 7.** Cardiotoxicity data of cod larvae exposed to MGO500 (green), MGO1000 (blue) and IFO (red) as a function of exposure concentration (µg/L TEM). A: Heart rate. B: Silent ventricle severity. C: Pericardial oedema severity. Data given as average ± SEM ($N = 28 - 32$). Control values are given as grey line (broken line: SEM, $N = 45$). No indications of silent ventricle (B) or pericardial oedema (C) were observed in controls.
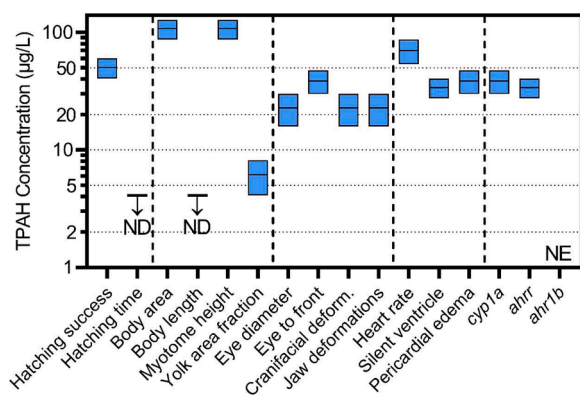
### 3.8. Effect limits

The most sensitive parameters responding to the exposure were related to growth and development (hatching time, standard length and yolk sac fraction). When related to exposure concentrations, there were only minor differences between the three WAFs. Effect limits for each recorded parameter is therefore indicated as the range between the highest concentration with no significant effect concentration (NOEC) and the lowest effect concentration (LOEC) on data pooled from all three oils (Fig. 8). For three of the recorded parameters (hatching time, length and yolk sac area fraction), significant effects were observed at the lowest exposure concentration for all three fuel oils and NOEC could not be determined. Whereas effects on growth (reduced body length) and hatching time extended to below 4.1 µg/L TPAH, a significant increase

in deformations were observed in the range of 15 – 47 µg/L TPAH. Effect limits for effects on heart anomalies and induction of *cyp1a* and *ahrr* transcripts were in the range of 27 – 40 µg/L TPAH. Corresponding data for TEM are given in Fig. S9.1 (SI 9). Statistical output and effect limits for all parameters and endpoints are given in Table S9.1 (SI 9).

## 4. Discussion

### 4.1. Chemical characterization of fuel oil LE-WAFs

The LE-WAFs of the three fuel oils differ in their chemical composition and total WAF concentrations measured as the sum of volatile organic components (VOC, C5 - C9) and total extractable material (TEM) differed significantly. Overall, the MGO1000 fuel oil displayed the

**Fig. 8.** Ranges of effect limits (μg/L TPAH) for WAFs based on pooled data from all three fuel oils. Effect parameters except for hatching were recorded 3 days post hatch of the control group. Estimated ranges for effect limits are shown as the range between the lowest concentration showing significant effects (LOEC) and the highest recorded concentration with no significant effect (NOEC). ND = no effect limit detected (significant response at lowest concentration), NOEC determined, NE = no effect observed.

highest concentrations of most identified/resolved and unresolved (UCM) components. This is in line with previous reports on the solubility of fuel oil components (Faksness and Altin, 2017).

### 4.2. Phenotypic outcomes of fuel oil exposure during embryogenesis

Exposure of cod embryos to WAFs of fuel oils induced a wide range of toxic effects. Within the TPAH concentration range used (4.1 - 128 μg/L TPAH), we observed reduced hatching success, premature hatching, increased mortality, smaller larvae, increased yolk fraction, jaw and craniofacial deformations, and cardiac toxicity in hatchlings; mostly in a concentration-dependant manner for the three fuel oils tested. Cold-water fish species are sensitive to petrogenic exposure during embryogenesis, as have previously described for crude oils (Hansen et al., 2018a, 2019a; Incardona et al., 2009; Laurel et al., 2019; Sørensen et al., 2017; Sørhus et al., 2015, 2016) and produced water (Hansen et al., 2019b). Even the lowest concentration used in our experiments (4.1 μg/L TPAH), significant effects were observed on the timing of hatch, larvae body length and yolk sac fraction. Comparable exposure concentrations, reported by Sørhus et al. (2015), caused reduced heart rate, reduced hatching success, larvae mortality and increased *cyp1a* expression in the Atlantic haddock. Lower exposure concentrations (0.65 - 1.1 μg/L TPAH) caused reduced larvae size and altered lipid metabolism in polar cod (*Boregadus saida*) (Laurel et al., 2019). Capelin (*Mallotus villosus*) embryos exposed to 40 μg/L TPAH also displayed increased embryonic mortality and hatching success, however, surviving larvae did not suffer the same morphological effects (yolk sac oedema, pericardial oedema, craniofacial deformations and altered hatch timing) (Frantzen et al., 2012) as have been observed in cod, haddock and polar cod at comparable exposure concentrations. In our study, where we imaged larvae on the same day of post fertilization (17 dpf) for all groups, we expected that exposure groups that hatched prematurely would display larvae with longer and larger body size and smaller yolk sacs, compared to controls and those that hatched up to 4 days later. However, this was not the case.

### 4.3. Changes in ahr gene battery in relation to phenotypic outcomes

The activation of Ahr and subsequent induction of Cyp1a have been historically shown to affect the bioaccumulation, persistence, metabolite dynamics and toxic outcome of certain groups of chemicals in several organisms (Livingstone, 1998; Varanasi et al., 1987), including Atlantic cod exposed to oil (Hansen et al., 2016; Olsvik et al., 2011,

2012). Herein, we observed that the different fuel oils produced a concentration-dependant induction of *cyp1a* and *ahrr* mRNA, without a parallel increase in the expression of *ahr1b*. These findings are in accordance with previous studies showing that PAHs and their related compounds may induce *cyp1a* expression through the activation of Ahr (Chaloupka et al., 1995; Cheevaporn and Beamish, 2007; de Souza Anselmo et al., 2018). The discrepancy between *cyp1a/ahrr* and *ahr1b* might be related to multiple roles of *ahr* in physiology and development. As a transcription factor, the overall function of Ahr is not fully understood in teleost species, compared to mammals, where this protein has been reported to be constitutively expressed (Gu et al., 2000, 2020). Nevertheless, the Ahr and Ahrr belong to the bHLH class of transcription factors that interacts with each other to form heterodimers (Avilla et al., 2020; Josyula et al., 2020). Comparative genomic analyses have demonstrated that the *ahr* gene battery are highly diversified in non-mammalian vertebrates, compared to mammalian species (Hahn et al., 2006). In fish, the expression of *ahr* genes vary, showing the *ahr2* as the most abundant with broader tissue distribution, while the *ahr1* is mainly expressed in the brain and heart (Hansson et al., 2004; Karchner et al., 2006). In cod, it was hypothesized that the Ahr has assumed a broader compensatory functional role as a xenosensor (Eide et al., 2018), suggesting higher diversity and functional properties of the Ahr signalling pathway in cod (Aranguren-Abadia et al., 2020). Therefore, our analysis of *ahr1b* mRNA in whole-embryo homogenate might have missed the actual fuel oil mediated effects on this transcription factor in cod larvae.

Despite that the mechanism of Ahr signalling pathways affect cellular processes is not well-characterized, the roles of Ahr in regulating cell cycle has provided important clues on the role of Ahr ligands on cell proliferation, differentiation and apoptosis (Puga et al., 2005). Alteration of cardiovascular function, including physiological conditions such as anaemia, that either result due to a decrease in the total number of erythrocytes or reduction in the concentration of haemoglobin per erythrocyte in blood or a combination of both (Widmayer et al., 2006), are known to be affected by contaminants exposure (Olufsen and Arukwe, 2011; Watson et al., 2019). In general, changes in these functions reduce the uptake and distribution of oxygen in an organism, inhibiting growth and normal development of organs that rely on oxygen supply (Olufsen and Arukwe, 2011; Watson et al., 2019).

Further, effects on bone morphogenesis, such as alteration in craniofacial development, represent the initial and most vulnerable parameter of Ahr-ligand toxicity in fish models (Dong et al., 2012; Hornung et al., 1999; Olufsen and Arukwe, 2011; Teraoka et al., 2006; Watson et al., 2019). In the present study, while developmental, morphological and physiological parameters such as body area, standard length and myotome height, heart rate, silent ventricle, pericardial oedema and cranial deformations showed fuel oil concentration-dependant alterations, the changes in molecular drivers of these alterations (*vegfaa, runx2b, osteocalcin, col1a1a, col1a1b, ctsk, bmp4, bmp9* and *osterix*) did not directly parallel these effects. However, *vegfaa* showed apparent fuel oil type and concentration-specific modulations. A prevailing explanation for this discrepancy is that we used whole embryo homogenate for transcript expression analysis due to the difficulties in dissecting very small cod embryos, against the notion that the transcripts of these molecular drivers are shown to exhibit tissue-specific expression patterns (Dong et al., 2012; Van Wettere et al., 2013). Nevertheless, Olsvik and coworkers (2011), have previously reported that oil exposure increased and decreased the expression of transcripts that regulate bone resorption and formation, respectively, leading the authors to conclude that exposure of Atlantic cod larvae to oil affected biological processes related to cell differentiation and proliferation, apoptosis and tissue development.

Previous study has demonstrated the intra-strain differences in the sensitivity of early life stage to 2,3,7,8-tetrachlorodibenzo-p-dioxin (TCDD) exposure, showing dose-dependant decreases in cranial length, eye diameter, mass, and total length in viable swim-up rainbow

trout (Carvalho and Tillitt, 2004). In the absence of clear patterns in transcript changes, fuel oil effects on heart rate and cardiovascular function are interesting, since the process of ossification and angiogenesis are interconnected, and bone formation is dependant on systemic blood distribution (Murayama et al., 2019; Wu et al., 2019; Wuelling and Vortkamp, 2010). For example, Stevens and Williams (1999) reported that vascularization was observed before bone formation during development of bones and fracture healing. In addition, the induction of angiogenesis starts at the transition from preosteoblast to osteoblast, and cartilage scaffold is replaced by bone during endochondral bone formation which enables this transition to accompany blood vessel invasion (Filvaroff et al., 1999; Wuelling and Vortkamp, 2010) with subsequent regulation of *vegfaa* by hypoxia-inducible factor (Hif: a PAS protein family) and bone morphogenetic factor (Bmp) (Tzouvelekis et al., 2012; Whitehouse and Manzon, 2019). Previous studies have reported that a PAH (benzo(a)pyrene: BaP) altered the expression of *vegfaa* in knockout (Ahr-null) mice, with angiogenesis-related outcomes, suggesting that the expression of *vegf* is controlled by the Ahr (Ichihara et al., 2009; Whitehouse and Manzon, 2019). Elsewhere, exposure to TCDD reduced heart size and altered cardiac function in early life stages of rainbow trout (Hornung et al., 1999). Simultaneous expression of *ahr2* and *arnt* mRNA was shown to provide protection against TCDD-mediated changes in heart morphology, reduced number of cardiac myocytes, decreased cardiac output and ventricular standstill in zebrafish larvae (Antkiewicz et al., 2006).

In a different study, it was demonstrated that exposure to TCDD (a strong Ahr agonist), altered erythropoiesis with a decrease in blood flow, and this effect did not translate to observable defects in blood vessel structure in zebrafish fry (Antkiewicz et al., 2005; Belair et al., 2001; Carney et al., 2006). Overall, our data showing that fuel oils modulated *ahr1b, vegfaa* and *ahrr* expressions, however, associated alterations of phenotypic outcomes related to craniofacial and cardiovascular deformations are not directly comparable, probably due to the complex chemical composition of the fuel oil types (see below). Elsewhere, the roles of Ahr in the alteration of cardiac functions were validated in a study by Billiard et al. (2006) showing that *ahr2* knockdown, reduced cardiac toxicity in combined b-naphthoflavone (BNF: a PAH-type Ahr agonist) and a-naphthoflavone (ANF: a Cyp1a inhibitor) exposure to zebrafish embryos. The authors proposed that these findings were in accordance with previous induction and inhibition experiments, suggesting that the underlying mechanisms of the developmental toxicity of PAH-type Ahr agonists may differ from those of planar halogenated aromatic hydrocarbons (Billiard et al., 2006). Regardless, it should be noted that the fuel oils used in the present study contained a complex mixture of chemicals. Therefore, the identification of potential pathways of PAH toxicity in developing fish embryos, in combination with fuel oil characterization, represent a robust, chemical and mechanistic-based approach for assessing risk of complex mixture of environmental contaminants in the Arctic.

### 4.4. Effects on angiogenesis and osteogenic differentiation

It is known that *vegfaa* is the main activator of angiogenesis in body areas that suffer from oxygen deprivation (Breen et al., 2008; Cannon et al., 2019; Dery et al., 2005). In addition, the inhibition of vascular development can critically affect growth and development due to diminished oxygen levels (Cannon et al., 2019; Miller and Johnson, 2017). Given the crosstalk within the PAS protein family, and their intricate relationships with *vegfaa* and *bmp*, exposure to complex mixture of fuel oil components will potentially compromise development and detoxification (Ding et al., 2006; Dornberger et al., 2016), as demonstrated in the present study. Thus, we propose, as a possible mechanism, that anaemia may produce cellular starvation for oxygen (i. e., hypoxic condition), that subsequently activates the expression of *vegfaa* to drive angiogenesis.

During bone development, mesenchymal stem cells differentiate into chondrocytes through a process that is tightly regulated by Sox9, with subsequent downstream effect that is regulated by *col2a1* (Huang et al., 2020; Yao et al., 2018). Osteochondroprogenitors that are derived from mesenchymal stem cells express *sox9* (Yao et al., 2018) and *runx2* (Ma et al., 2019), as their main transcription factors, during condensation of skeletal anlagen. A balance between *sox9* and *runx2*, drives the differentiation of osteochondroprogenitor in chicken embryos, where overexpression of *sox9* and *runx2* induce chondrogenesis and osteogenesis, respectively (Ma et al., 2019). However, *sox9* was demonstrated to dominate over *runx2* in mesenchymal precursors going through a chondrogenic lineage during endochondral ossification (Ma et al., 2019; Zhou and Ogata, 2013). As mentioned earlier, the expression pattern of *runx2b, col1a1a, col1a1b, osteocalcin, ctsk, bmp4, bmp9* and *osterix* did not show a direct fuel oil type or concentration-dependant alterations, as observed for *cyp1a* and *ahrr*. We proposed that this is presumably due to local changes in expression pattern of these transcripts that were possibly masked by whole egg RNA isolation. It was previously suggested that the Atlantic cod follows a sequence of cranial ossification that is generally conserved in most fish species (Sæle et al., 2017), suggesting that these sequential events might be transiently and differentially affected by exposure to contaminants, including fuel oil as tested in the present study. However, considering these molecular processes in bone formation and observed deformations and cardiovascular alterations, and that the expression of transcripts involved in ossification process were not significantly affected, our findings suggest that the effects on ossification activity may originate from either endochondral or intramembranous ossification processes (Vaes et al., 2006).

### 4.5. Toxicity thresholds and environmental risk assessment

Understanding the underlying mechanisms by which fuel oils elicit detrimental impact on fish embryos is important for assessing long-term consequences of accidental fuel oil spills in the environment. Our study suggests that the tested fuel oils displayed similar mechanisms of toxicity by activating the Ahr gene battery (*cyp1a* and *ahrr*) that further triggered the developmental effects on ELS of fish. These findings are in accordance with previous observations in fish exposed to crude oils (Incardona, 2017). To assess toxicity thresholds of crude oils, water concentrations of TPAH are most often used as a basis. In environmental risk assessment, toxicity thresholds (NOEC, LOEC, EC$_{50}$, LC$_{50}$) are widely used. The use of NOEC and LOEC as we have used here for establishing toxicity thresholds limits, has been rightfully criticised for being extremely influenced by experimental design. However, to be able to compare thresholds for the various effect parameters, we found this was the best way to visualize the ranges of expected effect limits. For most of the transcripts studied in the present study, we observed a lack of clear dose-response, restricting the establishment of NOEC/LOEC. Toxicity thresholds for growth and development (hatching, larvae size and yolk sac fraction) were also below the lowest concentrations tested (4.1 µg/L TPAH/ 34 µg/L THC). The potential population impact of such effects is unclear, but it is suggested that smaller larvae with altered lipid metabolism, as observed in the present study, are less ability to survive over time (Laurel et al., 2019). Delayed mortality was also observed in cod larvae exposed to oil in a transient period during their first feeding period (Nordtug et al., 2011). Cardiac toxicity and craniofacial deformations, which inevitably will cause impaired blood circulation and inability to feed, occurred at higher concentrations in our experiment (range 16 to 47 µg/L TPAH / 132 to 542 µg/L THC).

The fuel oils tested contain a complex mixture of potential toxicants and the use of TPAH as a basis for establishing toxicity thresholds may therefore be inadequate. PAHs, particularly tricyclics, produce embryotoxicity in fish. However, when exposed as single PAHs, they thresholds for toxicity on a mass-basis are orders of magnitude higher, compared to when present in petrogenic mixtures (Incardona et al., 2004). This may in fact suggest that other unresolved petrogenic

components are significant contributors to the toxicity (Melbye et al., 2009; Sørensen et al., 2019). Literature has shown that relating toxicity to PAH concentrations underestimates toxicity in fish ELS tests (Barron et al., 1999; Barron and Holder, 2003). To improve risk and damage assessment of fuel oil spills, it is important to identify the components causing toxicity. Furthermore, exposures in the environment change dynamically resulting in fluctuating exposure concentrations on a temporal scale. For fish eggs to be affected by fuel oil components, toxic components need to be taken up from the water into the body. Thus, determination of exposure doses (body burdens) causing toxic effects is more relevant for determining the toxic potential of a spill than using water concentrations. Acquisition of relevant toxicokinetics model parameter, particularly bioconcentration factors and elimination rates, relevant for the toxicity-driving oil components and organisms at risk is needed. This will enable more realistic modelling approach to estimate impacts of fuel oil spills as it will account for fluctuations in exposure concentrations in the environment.

## Author statement

We, the authors, wish to confirm that there are no known conflicts of interest associated with this publication and there has been no significant financial support for this work that could have influenced its outcome.

We confirm that the manuscript has been read and approved by all named authors and that there are no other persons who satisfied the criteria for authorship but are not listed. We further confirm that the order of authors listed in the manuscript has been approved by all of us. Specified author contributions: Conceptualization: BHH, LGF, PSD and TN. Methodology: BHH, LGF, TN, JF, EAK, EO and AA. Software: BK and BHH. Analyses, validation and data curation: BHH, TN, JF, EAK, EO, BK, LGF, PSD, AA. Writing: BHH, AA, TN, LGF, EAK, LGF and PSD. Project administration: BHH. Funding acquisition: BHH.

We confirm that we have given due consideration to the protection of intellectual property associated with this work and that there are no impediments to publication, including the timing of publication, with respect to intellectual property. In so doing we confirm that we have followed the regulations of our institutions concerning intellectual property. We further confirm that any aspect of the work covered in this manuscript that has involved experimental animals has been conducted with the ethical approval of relevant bodies.

## Declaration of Competing Interest

The authors declare that they have no known competing financial interests or personal relationships that could have appeared to influence the work reported in this paper.

## Acknowledgments

## Supplementary materials

Supplementary material associated with this article can be found, in the online version, at doi:10.1016/j.aquatox.2021.105881.

## References

Antkiewicz, D.S., Burns, C.G., Carney, S.A., Peterson, R.E., Heideman, W., 2005. Heart malformation is an early response to TCDD in embryonic zebrafish. Toxicol. Sci. 84, 368–377.
Antkiewicz, D.S., Peterson, R.E., Heideman, W., 2006. Blocking expression of AHR2 and ARNT1 in zebrafish larvae protects against cardiac toxicity of 2,3,7,8-tetrachlorodibenzo-p-dioxin. Toxicol. Sci. 94, 175–182.
Aranguren-Abadia, L., Lille-Langoy, R., Madsen, A.K., Karchner, S.I., Franks, D.G., Yadetie, F., Hahn, M.E., Goksoyr, A., Karlsen, O.A., 2020. Molecular and functional properties of the atlantic cod (Gadus morhua) Aryl hydrocarbon receptors Ahr1a and Ahr2a. Environ. Sci. Technol. 54, 1033–1044.
Arukwe, A., 2006. Toxicological housekeeping genes: do they really keep the house? Environ. Sci. Technol. 40 (24), 7944–7949.
Arukwe, A., Nordtug, T., Kortner, T.M., Mortensen, A.S., Brakstad, O.G., 2008. Modulation of steroidogenesis and xenobiotic biotransformation responses in zebrafish (Danio rerio) exposed to water-soluble fraction of crude oil. Environ. Res. 107, 362–370.
Avilla, M.N., Malecki, K.M.C., Hahn, M.E., Wilson, R.H., Bradfield, C.A., 2020. The Ah receptor: adaptive metabolism, ligand diversity, and the Xenokine model. Chem. Res. Toxicol. 33, 860–879.
Barron, M., Podrabsky, T., Ogle, S., Ricker, R., 1999. Are aromatic hydrocarbons the primary determinant of petroleum toxicity to aquatic organisms? Aquat. Toxicol. 46, 253–268.
Barron, M.G., Heintz, R., Rice, S.D., 2004. Relative potency of PAHs and heterocycles as aryl hydrocarbon receptor agonists in fish. Marine Environ. Res. 58, 95–100.
Barron, M.G., Holder, E., 2003. Are exposure and ecological risks of PAHs underestimated at petroleum contaminated sites? Hum. Ecol. Risk Assess 9, 1533–1545.
Belair, C.D., Peterson, R.E., Heideman, W., 2001. Disruption of erythropoiesis by dioxin in the zebrafish. Dev. Dyn. 222, 581–594.
Billiard, S.M., Hahn, M.E., Franks, D.G., Peterson, R.E., Bols, N.C., Hodson, P.V., 2002. Binding of polycyclic aromatic hydrocarbons (PAHs) to teleost aryl hydrocarbon receptors (AHRs). Comp. Biochem. Physiol. B: Biochem. Mol. Bio. 133, 55–68.
Billiard, S.M., Timme-Laragy, A.R., Wassenberg, D.M., Cockman, C., Di Giulio, R.T., 2006. The role of the aryl hydrocarbon receptor pathway in mediating synergistic developmental toxicity of polycyclic aromatic hydrocarbons to zebrafish. Toxicol. Sci. 92, 526–536.
Breen, E., Tang, K., Olfert, M., Knapp, A., Wagner, P., 2008. Skeletal muscle capillarity during hypoxia: VEGF and its activation. High. Alt. Med. Biol. 9, 158–166.
Cannon, D.T., Rodewohl, L., Adams, V., Breen, E.C., Bowen, T.S., 2019. Skeletal myofiber VEGF deficiency leads to mitochondrial, structural, and contractile alterations in mouse diaphragm. J. Appl. Physiol. 127 (1985), 1360–1369.
Carney, S.A., Prasch, A.L., Heideman, W., Peterson, R.E., 2006. Understanding dioxin developmental toxicity using the zebrafish model. Birth Defect. Res. A Clin. Mol. Teratol. 76, 7–18.
Carvalho, P.S., Tillitt, D.E., 2004. 2,3,7,8-TCDD effects on visual structure and function in swim-up rainbow trout. Environ. Sci. Technol. 38, 6300–6306.
Chaloupka, K., Steinberg, M., Santostefano, M., Rodriguez, L.V., Goldstein, L., Safe, S., 1995. Induction of Cyp1a-1 and Cyp1a-2 gene expression by a reconstituted mixture of polynuclear aromatic hydrocarbons in B6C3F1 mice. Chem. Biol. Interact. 96, 207–221.
Cheevaporn, V., Beamish, F.W., 2007. Cytochrome P450 1A activity in liver and fixed wavelength fluorescence detection of polycyclic aromatic hydrocarbons in the bile of tongue-fish (Cynoglossus acrolepidotus, Bleeker) in relation to petroleum hydrocarbons in the eastern Gulf of Thailand. J. Environ. Biol. 28, 701–705.
de Souza Anselmo, C., Sardela, V.F., de Sousa, V.P., Pereira, H.M.G., 2018. Zebrafish (Danio rerio): a valuable tool for predicting the metabolism of xenobiotics in humans? Comp. Biochem. Physiol. C Toxicol. Pharmacol. 212, 34–46.
DeCola, E., Robertson, T., Fisher, M., Blair, L., 2018. Phasing Out the Use and Carriage for Use of Heavy Fuel Oil in the Canadian Arctic: Impacts to Northern Communities. Report to WWF-Canada [online]: Available from assets. wwf.ca/downloads/phasing_out_heavy_fuel_oil_report. pdf.
Dery, M.A., Michaud, M.D., Richard, D.E., 2005. Hypoxia-inducible factor 1: regulation by hypoxic and non-hypoxic activators. Int. J. Biochem. Cell Biol. 37, 535–540.
Ding, J., Li, J., Chen, J., Chen, H., Ouyang, W., Zhang, R., Xue, C., Zhang, D., Amin, S., Desai, D., Huang, C., 2006. Effects of polycyclic aromatic hydrocarbons (PAHs) on vascular endothelial growth factor induction through phosphatidylinositol 3-kinase/AP-1-dependent, HIF-1alpha-independent pathway. J. Biol. Chem. 281, 9093–9100.
Dong, W., Hinton, D.E., Kullman, S.W., 2012. TCDD disrupts hypural skeletogenesis during medaka embryonic development. Toxicol. Sci. 125, 91–104.
Dornberger, L., Ainsworth, C., Gosnell, S., Coleman, F., 2016. Developing a polycyclic aromatic hydrocarbon exposure dose-response model for fish health and growth. Mar. Pollut. Bull. 109, 259–266.
Eide, M., Rydbeck, H., Torresen, O.K., Lille-Langoy, R., Puntervoll, P., Goldstone, J.V., Jakobsen, K.S., Stegeman, J., Goksoyr, A., Karlsen, O.A., 2018. Independent losses of a xenobiotic receptor across teleost evolution. Sci. Rep. 8, 10404.
Esbaugh, A.J., Mager, E.M., Stieglitz, J.D., Hoenig, R., Brown, T.L., French, B.L., Linbo, T.L., Lay, C., Forth, H., Scholz, N.L., Incardona, J.P., Morris, J.M., Benetti, D.D., Grosell, M., 2016. The effects of weathering and chemical dispersion on Deepwater Horizon crude oil toxicity to mahi-mahi (Coryphaena hippurus) early life stages. Sci. Total Environ. 543, 644–651.
Faksnes, L.G., Altin, D., 2017. WAF and toxicity testing of diesel and hybrid oils. SINTEF Ocean, Trondheim 1–38.
Farkas, J., Nordtug, T., Svendheim, L.H., Amico, E.D., Davies, E.J., Ciesielski, T., Jenssen, B.M., Kristensen, T., Olsvik, P.A., Hansen, B.H., 2021. Effects of mine tailing exposure on early life stages of cod (Gadus morhua) and haddock (Melanogrammus aeglefinus). Environmental Research, p. 111447. https://doi.org/10.1016/j.envres.2021.111447.
Filvaroff, E., Erlebacher, A., Ye, J., Gitelman, S.E., Lotz, J., Heillman, M., Derynck, R., 1999. Inhibition of TGF-beta receptor signaling in osteoblasts leads to decreased bone remodeling and increased trabecular bone mass. Development 126, 4267–4279.

Fitzgibbon, A.W., Fisher, R.B., 1996. A Buyer's Guide to Conic Fitting. University of Edinburgh, Department of Artificial Intelligence.

Frantzen, M., Falk-Petersen, I.-.B., Nahrgang, J., Smith, T.J., Olsen, G.H., Hangstad, T.A., Camus, L., 2012. Toxicity of crude oil and pyrene to the embryos of beach spawning capelin (*Mallotus villosus*). Aquat. Toxicol. 108, 42–52.

Gomez-Duran, A., Carvajal-Gonzalez, J.M., Mulero-Navarro, S., Santiago-Josefat, B., Puga, A., Fernandez-Salguero, P.M., 2009. Fitting a xenobiotic receptor into cell homeostasis: how the dioxin receptor interacts with TGFbeta signaling. Biochem. Pharmacol. 77, 700–712.

Gu, C., Cai, J., Fan, X., Bian, Y., Yang, X., Xia, Q., Sun, C., Jiang, X., 2020. Theoretical investigation of AhR binding property with relevant structural requirements for AhR-mediated toxicity of polybrominated diphenyl ethers. Chemosphere 249, 126554.

Gu, Y.Z., Hogenesch, J.B., Bradfield, C.A., 2000. The PAS superfamily: sensors of environmental and developmental signals. Annu. Rev. Pharmacol. Toxicol. 40, 519–561.

Hahn, M.E., Karchner, S.I., Evans, B.R., Franks, D.G., Merson, R.R., Lapseritis, J.M., 2006. Unexpected diversity of aryl hydrocarbon receptors in non-mammalian vertebrates: insights from comparative genomics. J. Exp. Zool. A Comp. Exp. Biol. 305, 693–706.

Hansen, B.H., Farkas, J., Nordtug, T., Altin, D., Brakstad, O.G., 2018a. Does microbial biodegradation of water-soluble components of oil reduce the toxicity to early life stages of fish? Envir. Sci. Technol. 52, 4358–4366.

Hansen, B.H., Salaberria, I., Read, K.E., Wold, P.A., Hammer, K.M., Olsen, A.J., Altin, D., Øverjordet, I.B., Nordtug, T., Bardal, T., Kjørsvik, E., 2019a. Developmental effects in fish embryos exposed to oil dispersions – The impact of crude oil micro-droplets. Marine Environ. Res. 150, 104753.

Hansen, B.H., Sorensen, L., Carvalho, P.A., Meier, S., Booth, A.M., Altin, D., Farkas, J., Nordtug, T., 2018b. Adhesion of mechanically and chemically dispersed crude oil droplets to eggs of Atlantic cod (*Gadus morhua*) and haddock (*Melanogrammus aeglefinus*). Sci. Total Environ. 640-641, 138–143.

Hansen, B.H., Sørensen, L., Størseth, T.R., Nepstad, R., Altin, D., Krause, D., Meier, S., Nordtug, T., 2019b. Embryonic exposure to produced water can cause cardiac toxicity and deformations in Atlantic cod (*Gadus morhua*) and haddock (*Melanogrammus aeglefinus*) larvae. Marine Environ. Res. 148, 81–86.

Hansen, B.H., Størseth, T.R., Nordtug, T., Altin, D., Olsvik, P.A., 2016. Exposure of first-feeding cod larvae to dispersed crude oil results in similar transcriptional and metabolic responses as food deprivation. Journal of Toxicology and Environmental Health, Part A 79 (13–15), 558–571.

Hansson, M.C., Wittzell, H., Persson, K., von Schantz, T., 2004. Unprecedented genomic diversity of AhR1 and AhR2 genes in Atlantic salmon (*Salmo salar* L.). Aquat. Toxicol. 68, 219–232.

He, K., Gkioxari, G., Dollár, P., Girshick, R., 2017. Mask r-cnn. In: Proceedings of the IEEE International Conference on Computer Vision, pp. 2961–2969.

Hellstrøm, K., 2017. Weathering properties and toxicity of marine fuel oils - summary report, in: SINTEF (Ed.), pp. 1–82.

Hornung, M.W., Spitsbergen, J.M., Peterson, R.E., 1999. 2,3,7,8-Tetrachlorodibenzo-p-dioxin alters cardiovascular and craniofacial development and function in sac fry of rainbow trout (*Oncorhynchus mykiss*). Toxicol. Sci. 47, 40–51.

Huang, L., Zhang, L., Li, H., Yan, J., Xu, X., Cai, X., 2020. Growth pattern and physiological characteristics of the temporomandibular joint studied by histological analysis and static mechanical pressure loading testing. Arch. Oral. Biol. 111, 104639.

Ichihara, S., Yamada, Y., Gonzalez, F.J., Nakajima, T., Murohara, T., Ichihara, G., 2009. Inhibition of ischemia-induced angiogenesis by benzo[*a*]pyrene in a manner dependent on the aryl hydrocarbon receptor. Biochem. Biophys. Res. Commun. 381, 44–49.

Incardona, J.P., 2017. Molecular mechanisms of crude oil developmental toxicity in fish. Arch. Environ. Cont. Toxicol. 73, 19–32.

Incardona, J.P., Carls, M.G., Day, H.L., Sloan, C.A., Bolton, J.L., Collier, T.K., Scholz, N. L., 2009. Cardiac arrhythmia is the primary response of embryonic pacific herring (*Clupea pallasi*) exposed to crude oil during weathering. Env. Sci. Technol. 43, 201–207.

Incardona, J.P., Collier, T.K., Scholz, N.L., 2004. Defects in cardiac function precede morphological abnormalities in fish embryos exposed to polycyclic aromatic hydrocarbons. Toxicol. Appl. Pharmacol. 196, 191–205.

Incardona, J.P., Gardner, L.D., Linbo, T.L., Brown, T.L., Esbaugh, A.J., Mager, E.M., Stieglitz, J.D., French, B.L., Labenia, J.S., Laetz, C.A., Tagal, M., Sloan, C.A., Elizur, A., Benetti, D.D., Grosell, M., Block, B.A., Scholz, N.L., 2014. Deepwater Horizon crude oil impacts the developing hearts of large predatory pelagic fish. Proc. Natl. Acad. Sci. U. S. A. 111, E1510–E1518.

Incardona, J.P., Scholz, N.L., 2016. The influence of heart developmental anatomy on cardiotoxicity-based adverse outcome pathways in fish. Aquat. Toxicol. 177, 515–525.

Josyula, N., Andersen, M.E., Kaminski, N.E., Dere, E., Zacharewski, T.R., Bhattacharya, S., 2020. Gene co-regulation and co-expression in the aryl hydrocarbon receptor-mediated transcriptional regulatory network in the mouse liver. Arch. Toxicol. 94, 113–126.

Karchner, S.I., Franks, D.G., Kennedy, S.W., Hahn, M.E., 2006. The molecular basis for differential dioxin sensitivity in birds: role of the aryl hydrocarbon receptor. Proc. Natl. Acad. Sci. U. S. A. 103, 6252–6257.

Kvæstad, B, Hansen, B.H., Davies, E.J., submitted. Automated morphometrics on microscopy images of Atlantic Cod using Mask R-CNN and classical machine vision techniques. MethodsX. doi:MEX-D-21-00018 [210603-017609]. Submitted for publication.

Laurel, B.J., Copeman, L.A., Iseri, P., Spencer, M.L., Hutchinson, G., Nordtug, T., Donald, C.E., Meier, S., Allan, S.E., Boyd, D.T., Ylitalo, G.M., Cameron, J.R., French, B.L., Linbo, T.L., Scholz, N.L., Incardona, J.P., 2019. Embryonic crude oil exposure impairs growth and lipid allocation in a keystone arctic forage fish. iScience 19, 1101–1113.

Livingstone, D.R., 1998. The fate of organic xenobiotics in aquatic ecosystems: quantitative and qualitative differences in biotransformation by invertebrates and fish. Comp. Biochem. Physiol. A Mol. Integr. Physiol. 120, 43–49.

Lovdata, 2014. Forskrift om nasjonalparkene Sør-Spitsbergen, Forlandet og Nordvest-Spitsbergen, om naturreservatene Nordaust-Svalbard og Søraust-Svalbard, og om naturreservatene for fugl på Svalbard, in: miljødepartementet, K.-o. (Ed.).

Ma, L., Yang, Z.Q., Ding, J.L., Liu, S., Guo, B., Yue, Z.P., 2019. Function and regulation of transforming growth factor beta1 signalling in antler chondrocyte proliferation and differentiation. Cell. Prolif. 52, e12637.

Melbye, A.G., Brakstad, O.G., Hokstad, J.N., Gregersen, I.K., Hansen, B.H., Booth, A.M., Rowland, S.J., Tollefsen, K.E., 2009. Chemical and toxicological characterization of an unresolved complex mixture-rich biodegraded crude oil. Environ. Toxicol. Chem. 28, 1815–1824.

Miller, M.L., Johnson, D.M., 2017. Vascular development in very young conifer seedlings: theoretical hydraulic capacities and potential resistance to embolism. Am. J. Bot. 104, 979–992.

Murayama, A., Ajiki, T., Hayashi, Y., Takeshita, K., 2019. A unidirectional porous beta-tricalcium phosphate promotes angiogenesis in a vascularized pedicle rat model. J. Orthop. Sci. 24, 1118–1124.

Nepstad, R., Davies, E., Altin, D., Nordtug, T., Hansen, B.H., 2017. Automatic determination of heart rates from microscopy videos of early life stages of fish. J. Toxicol. Environ. Health, Part A 80, 932–940.

Nordtug, T., Olsen, A.J., Altin, D., Overrein, I., Storøy, W., Hansen, B.H., De Laender, F., 2011. Oil droplets do not affect assimilation and survival probability of first feeding larvae of North-East Arctic cod. Science of the total environment 412, 148–153.

Olsvik, P.A., Hansen, B.H., Nordtug, T., Moren, M., Holen, E., Lie, K.K., 2011. Transcriptional evidence for low contribution of oil droplets to acute toxicity from dispersed oil in first feeding Atlantic cod (*Gadus morhua*) larvae. Comparative Biochemistry and Physiology Part C: Toxicology & Pharmacology 154 (4), 333–345.

Olsvik, P.A., Lie, K.K., Nordtug, T., Hansen, B.H., 2012. Is chemically dispersed oil more toxic to Atlantic cod (Gadus morhua) larvae than mechanically dispersed oil? A transcriptional evaluation. BMC genomics 13 (1), 1–14.

Olufsen, M., Arukwe, A., 2011. Developmental effects related to angiogenesis and osteogenic differentiation in Salmon larvae continuously exposed to dioxin-like 3,3′,4,4′-tetrachlorobiphenyl (congener 77). Aquat. Toxicol. 105, 669–680.

Politis, S.N., Dahlke, F.T., Butts, I.A., Peck, M.A., Trippel, E.A., 2014. Temperature, paternity and asynchronous hatching influence early developmental characteristics of larval Atlantic cod, *Gadus morhua*. J. Exp. Mar. Biol. Ecol. 459, 70–79.

Prior, S., Walsh, D., 2018. A vision for a heavy fuel oil-free arctic. Environment: Sci. Policy Sustain. Dev. 60, 4–11.

Puga, A., Tomlinson, C.R., Xia, Y., 2005. Ah receptor signals cross-talk with multiple developmental pathways. Biochem. Pharmacol. 69, 199–207.

Sæle, Ø., Haugen, T., Karlsen, Ø., van der Meeren, T., Bæverfjord, G., Hamre, K., Rønnestad, I., Moren, M., Lie, K.K., 2017. Ossification of Atlantic cod (Gadus morhua)Developmental stages revisited. Aquaculture 524–533.

Scott, J.A., Incardona, J.P., Pelkki, K., Shepardson, S., Hodson, P.V., 2011. AhR2-mediated, CYP1A-independent cardiovascular toxicity in zebrafish (*Danio rerio*) embryos exposed to retene. Aquat. Toxicol. 101, 165–174.

Sørensen, L., Hansen, B.H., Farkas, J., Donald, C.E., Robson, W.J., Tonkin, A., Meier, S., Rowland, S.J., 2019. Accumulation and toxicity of monoaromatic petroleum hydrocarbons in early life stages of cod and haddock. Environ. Poll. 251, 212–220.

Sørensen, L., Sørhus, E., Nordtug, T., Incardona, J.P., Linbo, T.L., Giovanetti, L., Karlsen, Ø., Meier, S., 2017. Oil droplet fouling and differential toxicokinetics of polycyclic aromatic hydrocarbons in embryos of Atlantic haddock and cod. PLoS ONE 12, e0180048.

Sørhus, E., Edvardsen, R.B., Karlsen, Ø., Nordtug, T., Van Der Meeren, T., Thorsen, A., Harman, C., Jentoft, S., Meier, S., 2015. Unexpected interaction with dispersed crude oil droplets drives severe toxicity in atlantic haddock embryos. PLoS ONE 10.

Sørhus, E., Incardona, J.P., Karlsen, Ø., Linbo, T., Sørensen, L., Nordtug, T., van der Meeren, T., Thorsen, A., Thorbjørnsen, M., Jentoft, S., Edvardsen, R.B., Meier, S., 2016. Crude oil exposures reveal roles for intracellular calcium cycling in haddock craniofacial and cardiac development. Sci. Rep. 6, 31058.

Stevens, D.A., Williams, G.R., 1999. Hormone regulation of chondrocyte differentiation and endochondral bone formation. Mol. Cell Endocrinol. 151, 195–204.

Suzuki, S., 1985. Topological structural analysis of digitized binary images by border following. Comput. Vis. Graphic. Image Process. 30, 32–46.

Teraoka, H., Dong, W., Okuhara, Y., Iwasa, H., Shindo, A., Hill, A.J., Kawakami, A., Hiraga, T., 2006. Impairment of lower jaw growth in developing zebrafish exposed to 2,3,7,8-tetrachlorodibenzo-p-dioxin and reduced hedgehog expression. Aquat. Toxicol. 78, 103–113.

Tzouvelekis, A., Ntolios, P., Karameris, A., Koutsopoulos, A., Boglou, P., Koulelidis, A., Archontogeorgis, K., Zacharis, G., Drakopanagiotakis, F., Steiropoulos, P., Anevlavis, S., Polychronopoulos, V., Mikroulis, D., Bouros, D., 2012. Expression of hypoxia-inducible factor (HIF)-1a-vascular endothelial growth factor (VEGF)-inhibitory growth factor (ING)-4- axis in sarcoidosis patients. BMC Res. Notes 5, 654.

Vaes, B.L., Ducy, P., Sijbers, A.M., Hendriks, J.M., van Someren, E.P., de Jong, N.G., van den Heuvel, E.R., Olijve, W., van Zoelen, E.J., Dechering, K.J., 2006. Microarray analysis on Runx2-deficient mouse embryos reveals novel Runx2 functions and target genes during intramembranous and endochondral bone formation. Bone 39, 724–738.

Van Wettere, A.J., Law, J.M., Hinton, D.E., Kullman, S.W., 2013. Anchoring hepatic gene expression with development of fibrosis and neoplasia in a toxicant-induced fish model of liver injury. Toxicol. Pathol. 41, 744–760.

Varanasi, U., Stein, J.E., Nishimoto, M., Reichert, W.L., Collier, T.K., 1987. Chemical carcinogenesis in feral fish: uptake, activation, and detoxication of organic xenobiotics. Environ. Health Perspect. 71, 155–170.

Watson, A.T.D., Nordberg, R.C., Loboa, E.G., Kullman, S.W., 2019. Evidence for Aryl hydrocarbon receptor-mediated inhibition of osteoblast differentiation in human mesenchymal stem cells. Toxicol. Sci. 167, 145–156.

Whitehouse, L.M., Manzon, R.G., 2019. Hypoxia alters the expression of hif-1a mRNA and downstream HIF-1 response genes in embryonic and larval lake whitefish (*Coregonus clupeaformis*). Comp. Biochem. Physiol. A Mol. Integr. Physiol. 230, 81–90.

Widmayer, E.P., Raff, H., Strang, K.T., 2006. Vander's Human physiology: The mechanism of Body Functions, Tenth ed. McGraw Hill.

Wu, Y., Zhang, C., Wu, J., Han, Y., Wu, C., 2019. Angiogenesis and bone regeneration by mesenchymal stem cell transplantation with danshen in a rabbit model of avascular necrotic femoral head. Exp. Ther. Med. 18, 163–171.

Wuelling, M., Vortkamp, A., 2010. Transcriptional networks controlling chondrocyte proliferation and differentiation during endochondral ossification. Pediatr. Nephrol. 25, 625–631.

Yao, B., Zhang, M., Liu, M., Wang, Q., Liu, M., Zhao, Y., 2018. Sox9 functions as a master regulator of antler growth by controlling multiple cell lineages. DNA Cell Biol. 37, 15–22.

Zhang, T., Suen, C.Y., 1984. A fast parallel algorithm for thinning digital patterns. Commun. ACM 27, 236–239.

Zhou, L., Ogata, Y., 2013. Transcriptional regulation of the human bone sialoprotein gene by fibroblast growth factor 2. J. Oral Sci. 55, 63–70.